JACS
JOURNAL OF THE AMERICAN CHEMICAL SOCIETY
Communication
pubs.acs.org/JACS

Oxygen Reduction Catalysis at a Dicobalt Center: The Relationship of Faradaic Efficiency to Overpotential

Guillaume Passard, Andrew M. Ullman, Casey N. Brodsky, and Daniel G. Nocera*

Department of Chemistry and Chemical Biology, Harvard University, 12 Oxford Street, Cambridge, Massachusetts 02138, United States

Supporting Information

ABSTRACT: The selective four electron, four proton, electrochemical reduction of O_2 to H_2O in the presence of a strong acid (TFA) is catalyzed at a dicobalt center. The faradaic efficiency of the oxygen reduction reaction (ORR) is furnished from a systematic electrochemical study by using rotating ring disk electrode (RRDE) methods over a wide potential range. We derive a thermodynamic cycle that gives access to the standard potential of O_2 reduction to H_2O in organic solvents, taking into account the presence of an exogenous proton donor. The difference in ORR selectivity for H_2O vs H_2O_2 depends on the thermodynamic standard potential as dictated by the pK_a of the proton donor. The model is general and rationalizes the faradaic efficiencies reported for many ORR catalytic systems.

Renewable energy resources have the potential to impact climate change by mitigating carbon emissions attendant to a fossil based fuel infrastructure.[1,2] Solar energy may be stored in the form of chemical bonds and subsequently recovered on demand in the form of electricity by using fuel cells.[3,4] The cathodic $4e^-$, $4H^+$ oxygen reduction reaction (ORR) of hydrogen-based fuel cells is kinetically challenging, and overall energy conversion efficiencies depend on the selective production of H_2O. Platinum can meet the demanding criteria of efficient ORR,[3,5] but the metal is critical, spurring efforts to develop catalysts based on earth abundant transition metals such as cobalt[6−10] and iron.[11−18] ORR in such systems is often performed in nonaqueous solution using a strong acid (e.g., trifluoroacetic acid (TFA), protonated *N*,*N*-dimethylformamide (DMF-H^+), or perchloric acid) as the proton donor.[14,15,19,20] In assessing activity, we and others often employ the faradaic efficiency for H_2O production as a performance benchmark.[14,19,20] However, faradaic efficiency is difficult to interpret in the absence of a thermodynamic potential that correctly accounts for the activity of the proton in nonaqueous solution.

Dicobalt complexes in acetonitrile (MeCN) and in the presence of O_2 and strong acid demonstrate excellent faradaic efficiencies for H_2O production.[21] We have prepared the pair of dicobalt complexes shown in Scheme 1 wherein a diamond $Co(III)_2(OH)_2$ core is stabilized by the six coordinate ligand, dipyridylethane naphthyridine (DPEN). The complex is similar to the first row metal complexes of DPEN (and its fluorinated analogue, DPFN) prepared by Tilley and co-workers[22−24] excepting the anionic bridging ligand. This dicobalt motif is useful because it is soluble in water and nonaqueous solutions and affords access to a wide range of overpotentials and faradaic efficiencies for ORR. We now develop a general framework to shed light on (a) how solvent and acid strength affect the overpotential of ORR catalysis and (b) the correlation between ORR overpotential and faradaic efficiency.

Scheme 1. Dicobalt Complexes Composed of a $Co(III)_2(OH)_2$ Diamond Core Stabilized by a DPEN Ligand with Anionic Acetamidate (1) and Acetate (2) Bridging Ligands

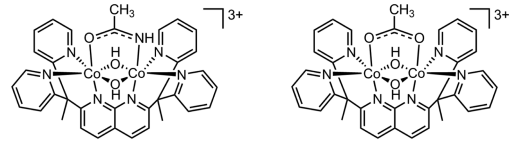

$[Co_2(OH)_2DPEN(\mu\text{-}1,3\text{-}OC(NH)CH_3)]^{3+}$ **1**

$[Co_2(OH)_2DPEN(\mu\text{-}1,3\text{-}OAc)]^{3+}$ **2**

Complex **1** was prepared by the addition of the DPEN ligand to $Co(NO_3)_2$ in a 1:1 water/acetone mixture. Air oxidation to furnish the two Co(III) centers is slow; thus H_2O_2 was used to drive the oxidation. The bridging acetamidate ligand was furnished by heating MeCN solutions of the PF_6 salt of the dicobalt complex. Complex **2** was prepared in a similar fashion, except using a $Co(OAc)_2$ precursor salt to furnish the bridging acetate ligand. The compounds were characterized by NMR, mass spectrometry, and elemental analysis (see SI for details).

Figure 1 shows CVs of **1** and **2** in MeCN in the absence of O_2 (red trace). The reversible CV wave corresponds to the

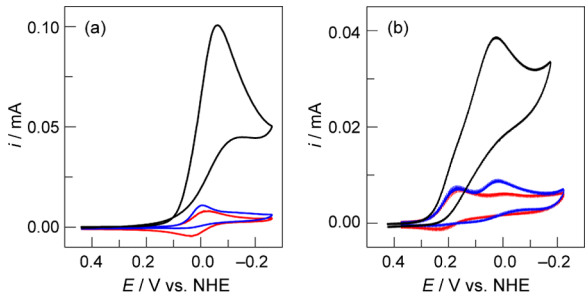

Figure 1. Cyclic voltammetry of (a) **1** and (b) **2** in MeCN (0.1 M *n*-Bu_4NPF_6) under Ar (red) and O_2 (blue), and in the presence of 50 mM AcOH (black); v = 0.1 V s^{-1}.

Received: December 8, 2015
Published: February 13, 2016

DOI: 10.1021/jacs.5b12828
J. Am. Chem. Soc. 2016, 138, 2925−2928

Co_2(III,III)/Co_2(III,II) couple; redox processes of the DPEN ligand occur at a very negative potential (Figure S1). Consistent with the poorer electron-donating property of the acetate bridge, the Co_2(III,III)/Co_2(III,II) couple for **2** is shifted anodically by 250 mV as compared to that of **1**. The presence of O_2 (8.1 mM) causes a loss of reversibility for the Co_2(III,III)/Co_2(III,II) wave (blue trace, Figure 1) and concomitant slight increase in current. This loss of reversibility is a clear indication that O_2 binds to complexes **1** and **2** following the one-electron reduction of the dicobalt core. Whereas **1** exhibits a single reduction wave, **2** exhibits a small second wave that becomes more pronounced upon O_2 binding. In contrast to these small current−voltage perturbations of the complexes in the presence of O_2, addition of acetic acid (AcOH) to **1** and **2** in the presence of O_2 results in a single large reduction wave. Such a significant increase in current is consistent with a catalytic ORR process. The need for both AcOH and O_2 to engender the large current indicates that protons are necessary for catalytic ORR turnover. Moreover, the current increase exhibits a dependence on the amount of AcOH (Figure S2), which confirms the implication of protons in the mechanism of ORR. At the highest acid concentrations, the foot of the catalytic wave shifts toward less negative potentials, demonstrating that the kinetics of the catalytic reaction improve with increasing acid concentration. With [AcOH] concentration in excess of 50 mM (Figure S2), the current decreases due to deactivation of the catalyst via acidolysis.

The products of ORR are typically water and hydrogen peroxide with the latter being the undesirable product owing to its lower cell voltage. Consequently, the design of ORR catalysts typically emphasizes the selectivity of H_2O vs H_2O_2 production. The commonly used metric for this selectivity is faradaic efficiency as measured by RRDE, for which the theory is very well-defined.[25] The faradaic yield is often determined arbitrarily at the potential for which the disk current is highest, though it is more representative to take into account the average yield throughout the entire catalytic region. The faradaic efficiency for H_2O_2 production as a function of potential may be determined by using

$$\%H_2O_2(E) = \frac{2i_r(E)/N}{i_d(E) + i_r(E)/N} \quad (1)$$

where $i_r(E)$ and $i_d(E)$ are the ring and the disk current, respectively, at potential E and N is the collection efficiency of the rotating ring disk electrode,[25] which was experimentally determined to be 0.26. The potential at the disk was scanned through the appropriate catalytic region while the potential at the ring was held at 1.17 V (all potentials are reported vs NHE) to ensure complete oxidization of H_2O_2. Figure 2a presents a representative experiment showing the ring and disk currents resulting from ORR of **1** in MeCN acidified with AcOH. Figure 2b shows the corresponding faradaic yield for H_2O_2 production across the potential range of ORR catalysis, obtained by application of eq 1 at different rotation rates. In applying eq 1, the average was taken over a potential range that gave a reliable measure of the current at the disk (i_d > 0.05 mA). Control experiments in the absence of catalyst show that there is no current on the ring regardless of the acid and its concentration within the limits of our potential window. Current from direct reduction of O_2 at the disk in the absence of catalyst occurs at more negative potentials (E_{disk} < −0.3 V vs NHE with strong acid to E_{disk} < −0.64 V vs NHE in the absence of acid). The faradaic efficiency should be the same at different rotation rates, unless

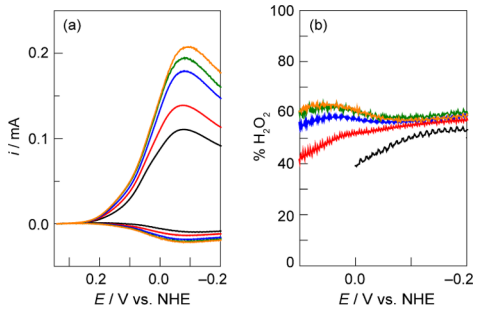

Figure 2. (a) Compound **1** (0.5 mM) in MeCN (0.1 M n-Bu_4PF_6) and AcOH (50 mM) under O_2 at different rotation rates: 100 (black), 250 (red), 500 (blue), 750 (green), and 1000 rpm (yellow). v = 0.02 V s^{-1}. Ring potential: 1.17 V. Disk current is positive, and ring current is negative. (b) Faradaic yield for H_2O_2 production obtained by application of eq 1 at different rotation rates.

hydrogen peroxide is an intermediate in the reaction leading to water. In this case, a decrease of the ring current would be observed with an increase in rotation rate. At a given potential, the ring and disk currents at various rotation rates show a small variance, however with no trend in rotation rate (Figure 2b). We attribute this variance (±10%) to arise in the collection efficiency. The average faradaic efficiency of H_2O production of 44% in Figure 2b was determined by taking 1 − [faradaic efficiency H_2O_2], which was determined as the average value across the entire trace for all rotation rates.

This RRDE study of ORR by **1** was expanded to include proton donors of different strength in MeCN (Figures S5−S8) and DMF (Figures S9 and S10) at different acid concentrations. The pK_a of the acids used in these studies are given in Table 1 in

Table 1. pK_a of Different Acids and Thermodynamic Standard Potential of O_2 Reduction to H_2O in MeCN and DMF

	MeCN		DMF	
acid, HA[a]	p$K_{a,HA}$	E^0/V vs NHE	p$K_{a,HA}$	E^0/V vs NHE
PhOH	27.2	0.430	18.8	−0.301
AcOH	22.3	0.720	13.3	0.020
ClAcOH	15.3	1.133	10.0	0.213
TFA	12.6	1.293	4.8	0.518

[a]Phenol (PhOH), acetic acid (AcOH), chloroacetic acid (ClAcOH), and trifluoroacetic acid (TFA).

DMF and MeCN.[26−29] For a given acid, the current increases and the foot of the wave shifts slightly to more positive potentials with acid concentration (e.g., Figure S2). These observations indicate that the effect of acid concentration is rooted in the kinetics of ORR. Most significantly, the H_2O yield in organic solvents increases with increasing acid strength. Figure 3a plots the average faradaic efficiency of H_2O for the different acids using eq 1. We note that the faradaic efficiency changed minimally with acid concentration (Table S1) over a range where acidolysis of the compound was minimal (≤50 mM acid concentration). As shown in Figure 3a, the faradaic efficiency varies substantially with pK_a (e.g., **1** with TFA in MeCN gives an average faradaic efficiency for H_2O production of 96% as compared to 33% for the more weakly acidic phenol).

The dependence of ORR faradaic yield on the different acids can be explained by considering the thermodynamic standard potential of the reduction of O_2 to H_2O as a function of acid pK_a (Table 1). We have developed a thermodynamic cycle akin to

DOI: 10.1021/jacs.5b12828
J. Am. Chem. Soc. 2016, 138, 2925−2928

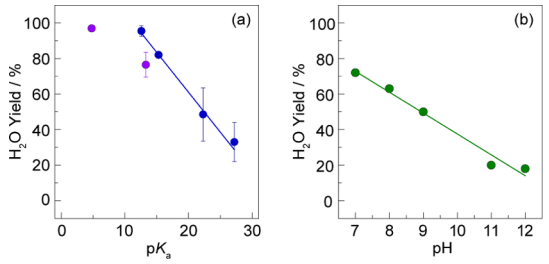

Figure 3. (a) Faradaic efficiency of **1** toward H_2O production as a function of acid pK_a of different acids listed in Table 1 in MeCN (blue) and DMF (green). (b) Faradaic efficiency of **1** toward H_2O production as a function of solution pH adjusted by aqueous phosphate buffer.

that developed by Costentin et al. for CO_2 reduction to CO (Scheme S1).[30] Using this cycle, the standard potential is given by

$$E^0_{O_2/2H_2O,HA,S} = E_{J,S} + E^0_{O_2/2H_2O,aq} - \frac{4\Delta G^0_{H^+,S\to aq} - 2\Delta G^0_{H_2O,S\to aq}}{2F} - \frac{RT\ln 10}{F} pK_{a\,HA,S} \quad (2)$$

where eq 2 accounts for the standard potential of ORR to furnish H_2O in solvent S and in the presence of HA ($E^0_{O_2/2H_2O,HA,S}$) from that in aqueous solution $E^0_{O_2/2H_2O,aq}$, corrected for the interliquid junction potential, $E_{J,S}$, between water and solvent S. The terms in eq 2 are defined within Scheme S1. Substituting the constants in eq 2 for MeCN and DMF, respectively, yields

$$E^0_{O_2/2H_2O,MeCN} = 2.038 - \frac{RT\ln 10}{F} pK_{a,HA,MeCN} \quad (3)$$

$$E^0_{O_2/2H_2O,DMF} = 0.799 - \frac{RT\ln 10}{F} pK_{a,HA,DMF} \quad (4)$$

We note that these equations contain no term for acid concentration, which is reflected in the lack of a noticeable concentration effect on selectivity (Table S1). For the case of water, the standard potential evolves with pH in a standard fashion:

$$E^{0'}_{O_2/2H_2O,aq} = E^0_{O_2/2H_2O,aq} - \frac{RT\ln 10}{F}\mathrm{pH} = 1.23 - \frac{RT\ln 10}{F}\mathrm{pH} \quad (5)$$

From eqs 3 and 4, we obtain the E^0 values presented in Table 1. These data reveal that the improved selectivity for H_2O production with increasing acid strength (Figure 3a) scales with the increasing standard potential of the ORR reaction for the different acids. Inasmuch as the applied potential to drive the ORR is defined by the reduction potential of the catalyst,

$$\Delta E_{ORR} = E^0_{O_2/2H_2O,HA,S} - E^0_{Co_2(III,III)/Co_2(II,III)} \quad (6)$$

the faradaic efficiency scales with ΔE_{ORR}, which is the effective overpotential. Thus, the ORR pathway leading to the O−O bond cleavage needed to produce H_2O becomes favored in the presence of strong acid where there is a high effective overpotential. Conversely, with weak acids, the effective overpotential for ORR to H_2O is small, and the pathway leading to H_2O production is disfavored relative to H_2O_2.

The same trend of improved H_2O selectivity with stronger acid is observed in DMF solution (Figure 3a, navy circles). Whereas the faradaic efficiency for H_2O production in DMF and MeCN are similar, ORR may be driven at much lower effective overpotential in DMF owing to the significantly reduced value of $E^0_{O_2/2H_2O,HA}$ (arising from a difference in $G^0_{H^+,S\to aq}$, Table S2). Indeed, Figure S3 shows the typical catalytic CVs of **1** in MeCN and DMF. A shift of 650 mV is observed at the foot of the catalytic wave caused by the difference of 779 mV between the two standard potentials (see Table 1). Nonetheless this gain in terms of thermodynamics is somewhat offset in terms of kinetics, as the catalytic current in DMF is significantly reduced as compared to MeCN.

Experiments performed on **1** in water at different pHs lead to results (Figure S11) that are similar to those observed for ORR in nonaqueous solutions. The apparent standard potential decreases with pH according to eq 5, and accordingly, ΔE_{ORR} decreases with increasing pH. Concomitant with this lowering in the effective overpotential, the faradaic efficiency for H_2O production decreases (Figure 3b).

Changing the bridging anion from the acetamidate in **1** to acetate in **2** yields similar RRDE results in MeCN (Figures S12 and S13) and water (Figure S14). The trend of the average faradaic efficiency with pK_a in MeCN (Figure S15) and pH in water (Figure S16) is similar to that observed for ORR catalyst **1**. A positive shift of the catalytic wave is observed for **2** resulting in a decrease in ΔE_{ORR} and an attendant decrease in the effective ORR overpotential (Figure S4). This gain in terms of thermodynamics is offset in terms of kinetics, as the current at the maximum of the catalytic wave is smaller in **2** than **1** (Figure S14a).

Our studies establish that an increase in the effective overpotential of ORR (i.e., increased ΔE_{ORR}) is accompanied by an increase in faradic efficiency. Our model is general, and it applies to previously published ORR catalysts. Figure 4 shows a plot of reported faradaic efficiencies versus effective overpotential for **1** and **2** together with selected ORR catalysts

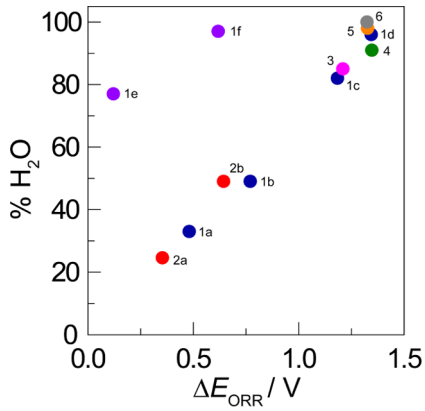

Figure 4. Faradaic efficiency for H_2O production vs ΔE_{ORR}($E^0_{O_2/2H_2O,HA,S} - E^0_{catalyst}$) for: **1** in MeCN (blue) with (1a) PhOH, (1b) MeCN, (1c) ClAcOH, (1d) TFA; **1** in DMF with (purple) (1e) AcOH, (1f) TFA; **2** in MeCN (red) with (2a) PhOH, (2b) AcOH; (3) Fe tetraphenylporphyrin in DMF with $HClO_4$ (pink), ref 15; (4) Fe *meso*-tetra(2-carboxyphenyl)porphine in MeCN with $(HDMF)^+$ (yellow), ref 14; (5) Fe *meso*-tetra(4-carboxyphenyl)porphine in MeCN with $(HDMF)^+$ (green), ref 14; (6) $Co^{III}_2(trpy)_2(\mu\text{-bpp})(\mu\text{-}1,2\text{-}O_2)]^{3+}$ (bpp = bis-(pyridyl)-pyrazolate, trpy = terpyridine) in MeCN with TFA (gray), ref 21.

DOI: 10.1021/jacs.5b12828
J. Am. Chem. Soc. 2016, 138, 2925−2928

operating in organic solvents.[14,15,21] As conveyed by eq 6, the effective overpotential, ΔE_{ORR}, is obtained by subtracting the standard reduction potential of each catalyst from the standard potential of O_2 reduction in a given solvent as determined from eq 2. We note the value of $\Delta G^0_{H^+,S\rightarrow aq}$ used in eq 2 has recently been re-examined;[31] whereas the various values of $\Delta G^0_{H^+,S\rightarrow aq}$ (Table S3) alter the absolute value of ΔE_{ORR}, the trend in Figure 4 is maintained. We have confined our analysis to ORR catalysts operating in DMF and MeCN, as the thermodynamic parameters needed for other solvent systems are unknown or poorly defined; thus literature examples such as those in acetone[20] and benzonitrile[19] are not included in our analysis. Additionally, the standard potential for solid state catalysts is unknown; hence, Figure 4 does not include solid state catalyst in the comparison.

The result of Figure 4 is striking inasmuch as very different catalysts with respect to metal and ligand type are undistinguished with regard to ORR faradaic efficiency. High faradaic efficiencies are obtained only at high effective overpotentials. Per the model embodied by eq 2, most studies achieve these high overpotentials by employing strong acids in nonaqueous solutions. In this regard, compound **1** appears to exhibit better performance in DMF, but this is not a result of better intrinsic catalyst activity, but due to a lowering of the effective overpotential (eq 4 as compared to eq 3) as a result of greater activity of the proton in DMF (Table S3). It is interesting to note that the reported faradaic efficiencies for most catalysts to date are indifferent to the kinetics of the ORR reaction. For instance, in compounds **4** and **5**, a proton relay group is positioned toward and away from a Fe porphyrin ring, respectively. Whereas the kinetics of the ORR are affected by the involvement of the proton relay,[14] the faradaic efficiency for the two compounds is similar as consequence of similar effective overpotentials.

In summary, we have developed a model that shows that ORR selectivity of catalysts is largely dictated by the effective overpotential. Our model reveals that in most systems reported to date, high ORR selectivities for H_2O is a result of large effective overpotentials for the reaction, achieved by the use of strong acids. The challenge to developing better ORR catalysts will be to maintain high catalytic efficiencies under conditions where the overpotential for ORR is greatly reduced.

■ ASSOCIATED CONTENT

Supporting Information

The Supporting Information is available free of charge on the ACS Publications website at DOI: 10.1021/jacs.5b12828.

Full experimental details and additional electrochemical data (PDF)

■ AUTHOR INFORMATION

Corresponding Author

*dnocera@fas.harvard.edu

Notes

The authors declare no competing financial interest.

■ ACKNOWLEDGMENTS

This work was supported by the U.S. Department of Energy Office of Science under Award Number DE-SC0009758. We also thank the TomKat Charitable Trust for support of this work. C.N.B. acknowledges the NSF's Graduate Research Fellowship Program. We are grateful to Prof. Cyrille Costentin for helpful discussions.

■ REFERENCES

(1) Lewis, N. S.; Nocera, D. G. *Proc. Natl. Acad. Sci. U. S. A.* **2006**, *103*, 15729.
(2) Lewis, N. S.; Nocera, D. G. *Bridge* **2015**, *46*, 41.
(3) Borup, R.; Meyers, J.; Pivovar, B.; Kim, Y. S.; Mukundan, R.; Garland, N.; Myers, D.; Wilson, M.; Garzon, F.; Wood, D.; Zelenay, P.; More, K.; Stroh, K.; Zawodzinski, T.; Boncella, J.; McGrath, J. E.; Inaba, M.; Miyatake, K.; Hori, M.; Ota, K.; Ogumi, Z.; Miyata, S.; Nishikata, A.; Siroma, Z.; Uchimoto, Y.; Yasuda, K.; Kimijima, K.; Iwashita, N. *Chem. Rev.* **2007**, *107*, 3904.
(4) Cook, T. R.; Dogutan, D. K.; Reece, S. Y.; Surendranath, Y.; Teets, T. S.; Nocera, D. G. *Chem. Rev.* **2010**, *110*, 6474.
(5) Steele, B. C. H.; Heinzel, A. *Nature* **2001**, *414*, 345.
(6) Anson, F. C.; Shi, C.; Steiger, B. *Acc. Chem. Res.* **1997**, *30*, 437.
(7) Kadish, K. M.; Shen, J.; Frémond, L.; Chen, P.; Ojaimi, M. E.; Chkounda, M.; Gros, C. P.; Barbe, J.-M.; Ohkubo, K.; Fukuzumi, S.; Guilard, R. *Inorg. Chem.* **2008**, *47*, 6726.
(8) Dogutan, D. K.; Stoian, S. A.; McGuire, R.; Schwalbe, M.; Teets, T. S.; Nocera, D. G. *J. Am. Chem. Soc.* **2011**, *133*, 131.
(9) Geiger, T.; Anson, F. C. *J. Am. Chem. Soc.* **1981**, *103*, 7489.
(10) McGuire, R., Jr; Dogutan, D. K.; Teets, T. S.; Suntivich, J.; Shao-Horn, Y.; Nocera, D. G. *Chem. Sci.* **2010**, *1*, 411.
(11) Collman, J. P.; Devaraj, N. K.; Decréau, R. A.; Yang, Y.; Yan, Y.-L.; Ebina, W.; Eberspacher, T. A.; Chidsey, C. E. D. *Science* **2007**, *315*, 1565.
(12) Collman, J. P.; Decréau, R. A.; Lin, H.; Hosseini, A.; Yang, Y.; Dey, A.; Eberspacher, T. A. *Proc. Natl. Acad. Sci. U. S. A.* **2009**, *106*, 7320.
(13) Collman, J. P.; Ghosh, S.; Dey, A.; Decréau, R. A.; Yang, Y. *J. Am. Chem. Soc.* **2009**, *131*, 5034.
(14) Carver, C. T.; Matson, B. D.; Mayer, J. M. *J. Am. Chem. Soc.* **2012**, *134*, 5444.
(15) Wasylenko, D. J.; Rodríguez, C.; Pegis, M. L.; Mayer, J. M. *J. Am. Chem. Soc.* **2014**, *136*, 12544.
(16) Chatterjee, S.; Sengupta, K.; Samanta, S.; Das, P. K.; Dey, A. *Inorg. Chem.* **2015**, *54*, 2383.
(17) Samanta, S.; Mittra, K.; Sengupta, K.; Chatterjee, S.; Dey, A. *Inorg. Chem.* **2013**, *52*, 1443.
(18) Samanta, S.; Das, P. K.; Chatterjee, S.; Sengupta, K.; Mondal, B.; Dey, A. *Inorg. Chem.* **2013**, *52*, 12963.
(19) Rosenthal, J.; Nocera, D. G. *Acc. Chem. Res.* **2007**, *40*, 543.
(20) Kakuda, S.; Peterson, R. L.; Ohkubo, K.; Karlin, K. D.; Fukuzumi, S. *J. Am. Chem. Soc.* **2013**, *135*, 6513.
(21) Fukuzumi, S.; Mandal, S.; Mase, K.; Ohkubo, K.; Park, H.; Benet-Buchholz, J.; Nam, W.; Llobet, A. *J. Am. Chem. Soc.* **2012**, *134*, 9906.
(22) Davenport, T. C.; Tilley, T. D. *Angew. Chem., Int. Ed.* **2011**, *50*, 12205.
(23) Davenport, T. C.; Tilley, T. D. *Dalton Trans.* **2015**, *44*, 12244.
(24) Davenport, T. C.; Ahn, H. S.; Ziegler, M. S.; Tilley, T. D. *Chem. Commun.* **2014**, *50*, 6326.
(25) Allen, J. Bard, L. R. F. *Electrochemical Methods: Fundamentals and Applications*, 2nd ed.; Wiley: New York, 2001.
(26) Andrieux, C. P.; Gamby, J.; Hapiot, P.; Savéant, J.-M. *J. Am. Chem. Soc.* **2003**, *125*, 10119.
(27) Costentin, C.; Evans, D. H.; Robert, M.; Savéant, J.-M.; Singh, P. S. *J. Am. Chem. Soc.* **2005**, *127*, 12490.
(28) Kütt, A.; Rodima, T.; Saame, J.; Raamat, E.; Mäemets, V.; Kaljurand, I.; Koppel, I. A.; Garlyauskayte, R. Y.; Yagupolskii, Y. L.; Yagupolskii, L. M.; Bernhardt, E.; Willner, H.; Leito, I. *J. Org. Chem.* **2011**, *76*, 391.
(29) Izutsu, K. *Acid-Base Dissociation Constants in Dipolar Aprotic Solvents*; Blackwell: Boston, 1990.
(30) Costentin, C.; Drouet, S.; Robert, M.; Savéant, J.-M. *Science* **2012**, *338*, 90.
(31) Pegis, M. L.; Roberts, J. A. S.; Wasylenko, D. J.; Mader, E. A.; Appel, A. M.; Mayer, J. M. *Inorg. Chem.* **2015**, *54*, 11883.

DOI: 10.1021/jacs.5b12828
J. Am. Chem. Soc. 2016, 138, 2925−2928